Geomechanics and Engineering, *Vol. 26, No. 4 (2021) 333-343*
https://doi.org/10.12989/gae.2021.26.4.333

An analytical model for radial consolidation prediction under cyclic loading

Monideepa Paul[1a], Kaustav Bakshi[2b] and Ramendu Bikas Sahu*[3]

[1]*Department of Civil Engineering, Heritage Institute of Technology, Kolkata-700107, India*
[2]*Department of Civil Engineering, Indian Institute of Technology Indore, Madhya Pradesh 452020, India*
[3]*Department of Civil Engineering, Jadavpur University, Kolkata- 700032, India*

(Received April 15, 2020, Revised May 17, 2021, Accepted August 4, 2021)

Abstract. The excess pore pressure increases under undrained cyclic loading which cause decrease in effective stress followed by possible failure in the soft soil. With the inclusion of vertical drains radial drainage allows quick dissipation of excess pressure during cyclic loading and thereby failure of foundation soil may be avoided. The present study aims for analytical closed-form investigation on soft cohesive deposit under radial flow consolidation through vertical drains with no smear when subjected to long-term rapid cyclic loading. The mathematical formulation of pore pressure including degree of consolidation under cyclic loading is developed by using Green's functions technique. Results obtained from the proposed formulation are in good agreement when compared with published field data which confirms its correctness to predict consolidation under cyclic loading. Once the proposed model is validated, it is applied to investigate the effect of vertical drains on variation of pore pressure ratio with number of loading cycles. The findings indicate that the pore water pressure generates slowly at the outermost boundaries of the vertical drains for initial number of loading cycles. The magnitude of pore water pressure accumulation increases and then dissipates for higher number of loading cycles. The variation of degree of consolidation for different frequencies of a unit cell of a prefabricated vertical drain is also furnished.

Keywords: cyclic stress ratio; effective confining pressure; frequency; number of cycles; plasticity index; pore water pressure; radial consolidation

1. Introduction

For construction of a structure on very thick saturated clay layers results into excess pore water pressure dissipation over long period of time. To accelerate the process of consolidation, vertical sand drains or prefabricated vertical drains (PVDs) can be installed at predetermined locations so that the water can drain out from the clay layer under superimposed load. Such observations were reported by Das (1985) and Smith and Smith (1998). Yoshikuni and Nakanodo (1974) included the effects of smear and well resistance for radial consolidation under static loading condition.

Such theories were continued to be studied and improved by many researchers like Indraratna and Redana (2000), Walker and Indraratna (2006), Lu *et al.* (2011) and Zhang *et al.* (2019). These authors proposed radial consolidation models for static load incorporating parametric variations like variable discharge capacity, equal strain with resistance.

The cohesive soil deposit below different civil engineering applications like highway, railway and runway embankments, ocean banks is subjected to rapid long-term cyclic loading [Yasuhara *et al.* (1995) and Samang *et al.* (2005)]. The consolidation theories developed for static loads predicted settlement for such soil deposit and the results differ significantly from the field measurements which indicate the requirement of consolidation studies under cyclic loads [Wilson and Elgohary (1974)]. The previous studies from Conte and Troncone (2006) and Ma *et al.* (2020) adopted low frequency cyclic loads but those were limited to one-dimensional consolidation along vertical direction only. Tang and Onitsuka (2000), Conte and Troncone (2009), Hsu and Liu (2013), Yazdani and Toufigh (2012), Deng *et al.* (2013), Kelly (2014), Amiri *et al.* (2018) studied consolidation through radial drainage by PVDs under linear time dependent loading considering well resistance and smear action. Zhu and Yin (2001), Leo (2004), Walker and Indraratna (2009) reported consolidation of soil along vertical and horizontal drainage under ramp load. Attya and Indraratna (2007), Indraratna *et al.* (2009, 2010 and 2016), Ni *et al.* (2014) conducted experimental investigation on cohesive soil and studied the pattern of pore water pressure generation under high frequency cyclic loading. Bai and Shi (2017) also reported experimental studies on consolidation behavior of saturated clay due to thermal loading cycles and observed significant volume reduction due to a series of heating – cooling cycles.

*Corresponding author, Professor
E-mail: sramendu@gmail.com
[a]Assistant Professor
E-mail: monideepapaul@gmail.com
[b]Assistant Professor
E-mail: bakshi.kaustav@gmail.com,
Kaustav.bakshi@iiti.ac.in

ISSN: 2005-307X (Print), 2092-6219 (Online)

The nonlinear theory proposed by Davis and Raymond (1965) led to a consolidation model based on void ratio and effective stress (e-log σ') which were adopted by many researchers. The model assumed the coefficient of consolidation as constant and it was noted that the compressibility and permeability tend to decrease with increasing effective stress for static load. Conte and Troncone (2007) proposed an expression for consolidation settlement as per Lancellotta (1995) based on Davis and Raymond (1965)'s assumption. It is highlighted that the excess pore pressure and degree of settlement with time factor differed from predicted results using linear theory when the external load was time dependent. Lekha *et al.* (1998), Li *et al.* (2018) reported a nonlinear theory based on effective stress / void ratio / permeability variations for radial consolidation of clayey soils under time dependent loading. These theoretical models considered cyclic loads as sinusoidal, haversine, ramp which are not the appropriate representation of the actual field condition. Hyodo *et al.* (1988) first reported a consolidation model under long-term cyclic loading and solved it numerically based on Terzaghi's basic consolidation theory. Paul and Sahu (2012), Paul *et al.* (2019) reported an analytical solution for one dimensional consolidation based on nonlinear theory proposed by Davis and Raymond (1965). However, there is no research report published on analytical solution of radial consolidation with vertical drains for long-term cyclic loading. Hence, the present paper aims to fill the void in the literature. The proposed study is expected to be helpful to the practicing civil engineers to predict consolidation behavior of foundation soil under long-term cyclic loads.

The present paper focuses on a generalized nonlinear radial consolidation model with no smear associated with undrained pore pressure generation model [Paul *et al.* (2015)] under long-term rapid cyclic loading. The proposed model incorporates the effects of confining pressure and in-situ stress directly. The effects of cyclic stress ratio (CSR), frequency of loading and plasticity index of soil are considered in this proposed model in an indirect manner. The solution estimates the model parameters more realistically as those values adopted here are from laboratory test results available in literature. The proposed model is expected to help the practicing engineers to predict settlements behavior of foundation soil during radial consolidation with vertical drains under long-term cyclic loading.

2. Framework of the model

Ni (2012) reported that the excess pore pressure generation for soil deposit under cyclic loading is slower when subjected to radial drainage compared to the undrained condition. Therefore, the excess pore water pressure generation under cyclic loading is the combined effect of undrained excess pore pressure generation and subsequent dissipation across the drainage boundary. Based on this concept, a radial consolidation model for no smear and no well resistance under cyclic loading is presented here.

The axisymmetric soil cylinder (Fig. 1) depicts d_e as the diameter of influence zone, a as the equivalent radius of the well (in case of PVD) and l as the thickness of consolidating soil layer. To derive the continuity equation in cylindrical coordinates a soil element shown in Fig. 2 is considered.

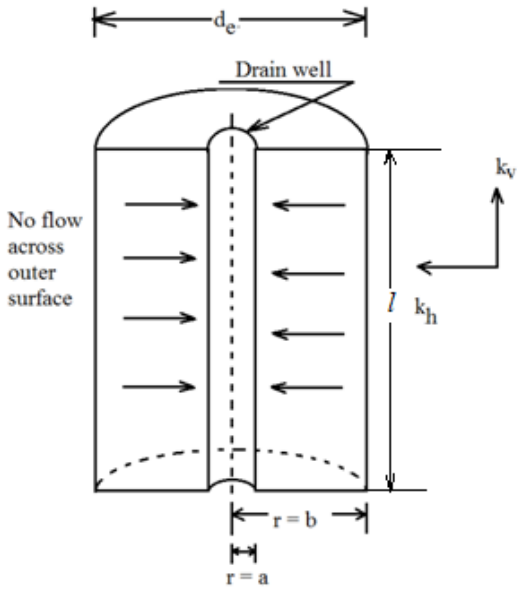

Fig. 1 Axisymmetric cylindrical soil sample

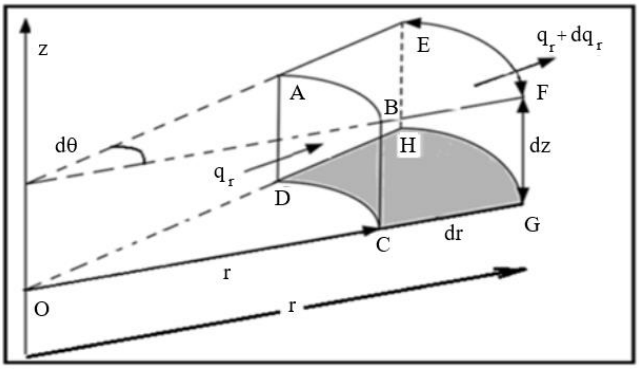

Fig. 2 Flow through soil element

The volume of the differential soil element is

$$dv = r \times dr \times d\theta \times dz \tag{1}$$

Mass of soil element is, $M = \rho \times dv$

Assuming that the water enters across the inner circumferential face ABCD has velocity v_r and density ρ. Therefore, the rate of mass (q_r) entering the soil element through ABCD is given as the following:

$$q_r = \rho v_r \times r \times d\theta \times dz \tag{2}$$

The rate of mass leaving the control volume through EFGH is given below,

$$q_r + dq_r = \left(\rho v_r + \frac{\partial(\rho v_r)}{\partial r} dr\right)(r + dr) \times d\theta \times dz \tag{3}$$

Now, the following equation can be written maintaining the continuity of flow.

Fluid entering through ABCD = (fluid accumulated or dissipated) + (Fluid leaving through EFGH)

The rate of accumulation or dissipation of fluid for the control volume $= \frac{\partial M}{\partial t}$,

$$\rho v_r \times r \times d\theta \times dz = \frac{\partial M}{\partial t} + \left(\rho v_r + \frac{\partial(\rho v_r)}{\partial r} dr\right)(r + dr) \times d\theta \times dz \quad (4)$$

The dr^2 in Eq. (4) can be neglected for being very small quantity.

Eq. (4) can be written as the following:

$$\frac{\partial M}{\partial t} + \frac{1}{r} \times \rho v_r \times r \times dr \times d\theta \times dz + \left(\frac{\partial}{\partial r}(\rho v_r) dr\right) \times r \times d\theta \times dz = 0 \quad (5)$$

Hence, final form of continuity equation in cylindrical coordinate system is given below,

$$\frac{\partial M}{\partial t} + \frac{1}{r} \times \rho v_r \times dv + \left(\frac{\partial(\rho v_r)}{\partial r}\right) \times dv = 0 \quad (6)$$

2.1 Mathematical formulation

For normally consolidated soil the void ratio (e) is related to effective vertical stress (σ′) as the following:

$$e = e_0 - C_c' \times \log_{10} \frac{\sigma'}{\sigma_0} \quad (7)$$

where, e_0 is the initial void ratio corresponding to stress σ_0', and C_c' is compression or re-compression index of the soil depending upon the nature of loading.

Differentiating void ratio (e) with respect to effective stress (σ′) the coefficient of volume change m_v (Lambe and Whitman, 1969) is found as the following:

$$m_v = \frac{0.434 \times C_c'}{(1 + e) \times \sigma'} \quad (8)$$

The variation of (1 + e) with time is quite less than the effective stress (σ′) during consolidation. Hence, (1 + e) is considered as constant for any load increment. Following Davis and Raymond's (1965) assumption Eq. (8) can be written as it is shown below,

$$m_{vr} = \frac{A_0}{\sigma'} \quad (9)$$

where, the constant A_0 is given as the following:

$$A_0 = \frac{0.434 \times C_c'}{(1 + e)} \quad (10)$$

For normally consolidated soils the coefficient of radial consolidation is $c_{vr} = k_h / (m_{vr} \times \gamma_w)$. Moreover, the rate of decrease in horizontal permeability (k_h) is proportional to the rate of decrease of compressibility in radial direction (m_{vr}). Thus, c_{vr} can be taken as constant.

From Darcy's law

$$v_r = k_h i = \frac{k_h}{\gamma_w} \cdot \frac{\partial u}{\partial r} \quad (11)$$

where, u is the pore water pressure.

Putting Eq. (11) in Eq. (6)

$$\frac{\partial M}{\partial t} + \frac{1}{r} \times \rho \times \left(\frac{k_h}{\gamma_w} \cdot \frac{\partial u}{\partial r}\right) \times dv + \left(\frac{\partial}{\partial r}\right) \times \left(\frac{k_h}{\gamma_w} \cdot \frac{\partial u}{\partial r}\right) \times \rho \times dv = 0 \quad (12)$$

Again,

$$c_{vr} = \frac{k_h}{\frac{A_0}{\sigma'} \gamma_w} \quad (13)$$

$$\frac{\partial M}{\partial t} + \frac{1}{r} \times \rho \times \left(m_{vr} c_{vr} \cdot \frac{\partial u}{\partial r}\right) \times dv + \left(\frac{\partial}{\partial r}\right) \times \left(m_{vr} c_{vr} \cdot \frac{\partial u}{\partial r}\right) \times \rho \times dv = 0 \quad (14)$$

Applying Eq. (13) into Eq. (14), we get the following:

$$\frac{\partial M}{\partial t} = -\left[\frac{1}{r} \cdot \frac{1}{\sigma'}\left(\frac{\partial u}{\partial r}\right) + \frac{1}{\sigma'} \cdot \frac{\partial^2 u}{\partial r^2} - \frac{1}{\sigma'^2}\left(\frac{\partial u}{\partial r} \cdot \frac{\partial \sigma'}{\partial r}\right)\right] \rho \times dv \times A_0 c_{vr} \quad (15)$$

The volumetric strain developed within the soil element is achieved by neglecting secondary compression or creep. It is shown as follows:

$$f = \frac{e - e_0}{1 + e_0} \quad (16)$$

$$f = \frac{C_c}{1 + e_0} \log_{10}\left(\frac{\sigma'}{\sigma'_0}\right) \quad (17)$$

It is taken up here that the rate of water lost per unit volume is equal to the rate of volume decrease per unit volume within a small element of soil.

$$\partial M = \partial f \times dv \times \rho \quad (18)$$

Here ∂f depicts the total volume strain, dv is the volume of soil element and ρ is the density of water,

Differentiating Eq. (18) with respect to time t, we get the following:

$$\frac{\partial M}{\partial t} = \frac{\partial f}{\partial t} \times dv \times \rho \quad (19)$$

Differentiating f with respect to time t,

$$\frac{\partial f}{\partial t} = \frac{C_c}{1 + e_0} \frac{0.434}{\sigma'} \left(\frac{\partial \sigma'}{\partial t}\right) \times dv \times \rho \quad (20)$$

Assuming $(1+e_0)$ is equal to (1+e), we get the following:

$$\frac{\partial f}{\partial t} = \frac{A_0}{\sigma'} \cdot \left(\frac{\partial \sigma'}{\partial t}\right) \times dv \times \rho \quad (21)$$

$$-\left[\frac{1}{r} \cdot \frac{1}{\sigma'}\left(\frac{\partial u}{\partial r}\right) + \frac{1}{\sigma'} \cdot \frac{\partial^2 u}{\partial r^2} - \frac{1}{\sigma'^2}\left(\frac{\partial u}{\partial r} \cdot \frac{\partial \sigma'}{\partial r}\right)\right] \rho \times dv \times A_0 c_{vr} = \frac{A_0}{\sigma'} \cdot \left(\frac{\partial \sigma'}{\partial t}\right) \times dv \times \rho \quad (22)$$

$$-\left[\frac{1}{r} \cdot \frac{1}{\sigma'}\left(\frac{\partial u}{\partial r}\right) + \frac{1}{\sigma'} \cdot \frac{\partial^2 u}{\partial r^2} - \frac{1}{\sigma'^2}\left(\frac{\partial u}{\partial r} \cdot \frac{\partial \sigma'}{\partial r}\right)\right] c_{vr} = \frac{1}{\sigma'} \cdot \left(\frac{\partial \sigma'}{\partial t}\right) \quad (23)$$

The long term cyclic loading considered in the present analysis is presented in Fig. 3.

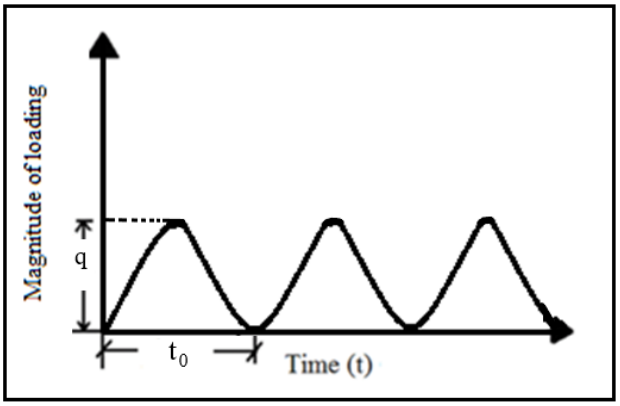

Fig. 3 Variation of loading with time relationship

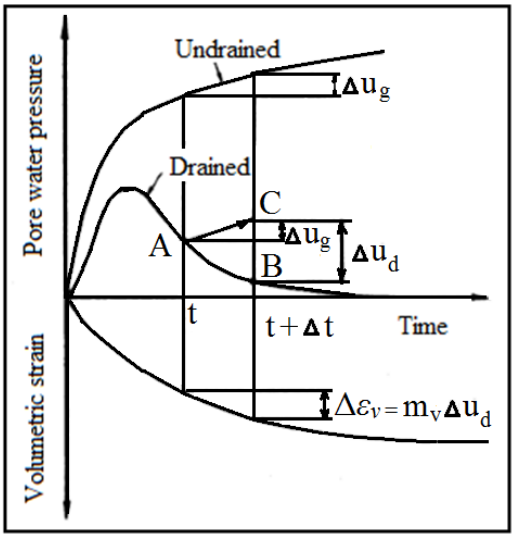

Fig. 4 A schematic diagram of undrained and partially drained behavior of soil under cyclic loading

From Terzaghi's principle of effective stress under cyclic loading condition, σ′ can be written as,

$$\sigma' = \sigma'_0 + \sigma_{cy} - u \tag{24}$$

σ'_0: Initial effective vertical stress in clay layer;

σ_{cy}: Amplitude of the cyclic deviator stress developed in consolidating clay layer;

u: Pore water pressure

The Eq. (24) for effective stress seems to be valid for low frequency cyclic loading such as oil tank, silos etc. However, the rapid high frequency load noted during wave propagation, high speed vehicular movement, the prediction of cyclic deviator stress is difficult both analytically and experimentally. On the other hand, the undrained pore pressure for cyclic loading can be predicted using the formulations reported by Paul *et al.* (2015) as a function of cyclic deviator stresses, number of cyclic loading, and plasticity of soil. Hyodo *et al.* (1988) found that a soil mass under to cyclic load with partially drained condition shows the pore water pressure first rises and then dissipates with time (Fig.4).

Fig. 4 shows that pore water pressure follows the path AB for an arbitrary time interval, t to (t +Δt) where Δt is time increment. The pore water pressure generation and dissipation during Δt is Δu_g and Δu_d, respectively. The resulting volumetric strain is $\Delta\varepsilon_v$. In case of long-term cyclic loading condition, the deformation is coupled with generation and dissipation of excess pore water pressure in the cohesive deposits.

Hence, it is appropriate to replace the cyclic deviator stress shown in Eq. (24) by the term generated pore pressure for soil under undrained condition. The corresponding expression for effective stress as proposed by Paul *et al.* (2019) as given below has been used in the present study.

$$\sigma' = \sigma'_0 + u_g - u \tag{25}$$

where, u_g is generated pore water pressure which is a function of number of cycles, frequency and magnitude of cyclic load expressed as cyclic stress ratio [CSR= $\sigma_{cyc}/\sigma'_{vc}$], confining pressure and plasticity index of soil. The cyclic stress ratio is defined by the ratio between the cyclic deviator stress, σ_{cyc}, to the initial effective overburden, σ'_{vc}. The u_g is expressed as shown below,

$$\frac{u_g}{\sigma'_{vc}} = f\left(CSR, N, \sigma'_{vc}, I_p\right)$$

Differentiating the above equation with respect to r and t, we get the following;

$$\frac{\partial \sigma'}{\partial r} = -\frac{\partial u}{\partial r} \tag{26}$$

and

$$\frac{\partial \sigma'}{\partial t} = \frac{\partial u_g}{\partial t} - \frac{\partial u}{\partial t} \tag{27}$$

$$\left(\frac{\partial u_g}{\partial t} - \frac{\partial u}{\partial t}\right) = -\left[\frac{1}{r}\cdot\left(\frac{\partial u}{\partial r}\right) + \cdot\frac{\partial^2 u}{\partial r^2} + \frac{1}{\sigma'}\left(\frac{\partial u}{\partial r}\right)^2\right] c_{vr} \tag{28}$$

Eq. (28) is the governing nonlinear equation for radial consolidation. As this equation is a function of r and t only, it does not account the changes of pore pressure with depth during consolidation.

Let us consider the following,

$$w = \ln\left(\frac{\sigma'}{\sigma'_f}\right) = \ln\left(\frac{\sigma'}{(\sigma'_0 + u_g)}\right) \tag{29}$$

σ'_f is final effective pressure $=(\sigma'_0 + u_g)$

Differentiating Eq. (29) with respected to the radial distance *r*, we get the following:

$$\frac{\partial w}{\partial r} = -\frac{1}{\sigma'}\cdot\left(\frac{\partial u}{\partial r}\right) \tag{30}$$

$$\frac{\partial^2 w}{\partial r^2} = -\frac{1}{\sigma'}\left(\frac{\partial^2 u}{\partial r^2} + \frac{1}{\sigma'}\left(\frac{\partial u}{\partial r}\right)^2\right) \tag{31}$$

Differentiating Eq. (29) with respected to time t,

$$\frac{\partial w}{\partial t} = \frac{1}{\sigma'}\cdot\left(\frac{\partial \sigma'}{\partial t}\right) \tag{32}$$

Substituting Eqs. (30), (31), and (32) into Eq. (28) leads to a simple differential equation in terms of 'w' which is shown as the following,

$$c_{vr}\left(\frac{\partial^2 w}{\partial r^2}+\frac{1}{r}\cdot\frac{\partial w}{\partial r}\right)=\left(\frac{\partial w}{\partial t}\right)+R(t) \quad (33)$$

where

$$R(t)=\frac{1}{(\sigma'_0+u_g)}\times\frac{\partial u_g}{\partial t}=\frac{1}{(\sigma'_0+u_g)}\times\frac{\partial u_g}{\partial N}\frac{\partial N}{\partial t} \quad (34)$$

and $\left(\frac{\partial N}{\partial t}\right)=\frac{1}{t_0}$

Here, R(t) = Source term of generated pore water pressure which is time dependent

N = Number of cycles

t_0 = Time period of the cyclic loading

3. Initial and boundary conditions

The initial and boundary conditions used to solve Eq. (33) are as follows:

$$\text{For } t=0 \text{ and } a\le r\le b;\ u=0 \text{ or } w=0 \quad (35)$$

$$\text{For } t>0 \text{ and } r=a;\ u=0 \text{ or } w=0 \quad (36)$$

$$\text{For } t>0 \text{ and } r=b;\ \frac{\partial u}{\partial r}=0 \text{ or } \frac{\partial w}{\partial r}=0 \quad (37)$$

3.1 A procedure for evaluation excess pore water pressure

For low amplitude cyclic loading, the excess pore water pressure under undrained condition initially increases at a certain rate and becomes asymptotic after certain number of cycles. Seed and Idriss (1971) and De Alba *et al.* (1976) conducted a number of undrained tests and proposed expressions of excess pore water pressure for potentially liquefiable sand deposits as a function of cyclic stress ratio. Van Eekelen and Potts (1978) and Matsui *et al.* (1980) reported a hyperbolic pattern of pore water pressure variation under cyclic loading. The authors considered the effects of plasticity index, over consolidation ratio (OCR) and other factors. A hyperbolic relation between the normalized excess pore pressures and number of cycles under cyclic shear strain was reported by Ohara and Matsuda (1988), Hyodo *et al.* (1988), Ansal and Erken (1989), Prakasha and Chandrasekaran (2005). These authors proposed models of undrained pore pressure under cyclic loading considering nature of soil, rate of loading, effective confining pressure, cyclic deviator stress, frequency and plasticity index. A generalized hyperbolic pattern was introduced by Paul *et al.* (2015) to obtain pore water pressure for varying load cycles, magnitude of cyclic deviator stress in terms 'CSR' and plasticity index related to soil consistency of cohesive deposits.

$$\frac{u_g}{\sigma'_0}=\left(\frac{N}{(A+B\times N)}\right)\left(\frac{1+2k_0}{3}\right) \quad (38)$$

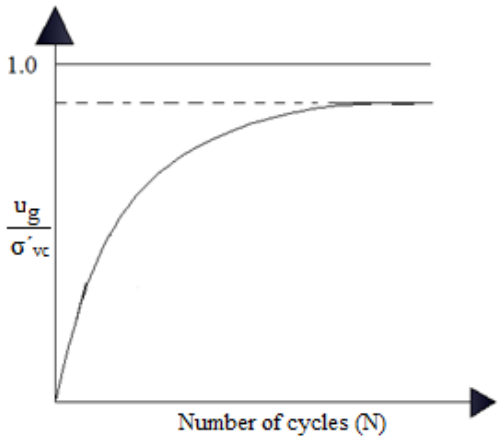

Fig. 5 A typical undrained pore water pressure generation model of soil

$$\because \sigma'_{vc}=\left(\frac{1+2k_0}{3}\right)\times\sigma'_0$$

where, N is the number of load cycle and A and B are stress dependent coefficients.

$$k_0=\sigma'_h/\sigma'_0$$

σ'_{vc} = effective confining pressure

σ'_0 = initial effective vertical stress

Here k_0 is the ratio of initial effective horizontal to vertical stresses.

The abovementioned expression is used to compute the pore water pressure under undrained condition.

Fig. 5 shows the functional relation between the pore pressure ratio and the number of cycles. The coefficient A is the inverse of the tangent to the curve drawn between pore pressure generation and number of load cycle at $u_g/\sigma'_{vc}=0$. The coefficient B is the inverse of the maximum pore pressure ratio.

4. Solution procedure

The mathematical formulation of this problem is given in Eq. (33)

$$\left(\frac{\partial^2 w}{\partial r^2}+\frac{1}{r}\cdot\frac{\partial w}{\partial r}\right)-\frac{1}{c_{vr}}R(t)=\frac{1}{c_{vr}}\left(\frac{\partial w}{\partial t}\right)$$

This differential equation can be solved by Green's functions [Carslaw and Jaeger (1959)]. To determine the appropriate Green's function, the homogeneous version of this mathematical formulation is given by,

$$\left(\frac{\partial^2 \psi}{\partial r^2}+\frac{1}{r}\cdot\frac{\partial \psi}{\partial r}\right)=\frac{1}{c_{vr}}\left(\frac{\partial \psi}{\partial t}\right) \quad (39)$$

$$\text{For } t=0,\quad \psi=F(r)=0 \text{ in the region at,}\quad a\le r\le b \quad (40)$$

$$\text{For } t>0,\quad \text{at } r=a,\quad \psi=0 \quad (41)$$

$$\text{For } t>0, \text{ at } r=b,\quad \frac{\partial \psi}{\partial r}=0 \quad (42)$$

Separating the variables, it can be shown that the solution for the time variable function is $(\exp^{-C_{vr}\beta_m{}^2 t})$, the space variable function $R_0(\beta_m, r)$ is the solution of the Eigen value problem which is written as the following:

$$\frac{\partial^2 R_0}{\partial r^2} + \frac{1}{r}\cdot\frac{\partial R_0}{\partial r} + \beta_m{}^2 R_0 = 0 \quad (43)$$

$$\text{For } t > 0, \text{ at } r = a,\ R_0 = 0 \quad (44)$$

$$\text{For } t > 0, \text{ at } r = b,\ \frac{\partial R_0}{\partial r} = 0 \quad (45)$$

The complete solution for ψ (r, t) is written as,

$$\psi(r,t) = \sum_{m=1}^{\infty} c_m \exp^{-c_{vr}\beta_m{}^2 t} R_0(\beta_m, r) \quad (46)$$

The application of the initial condition to Eq. (40) leads to the following:

$$F(r) = \sum_{m=1}^{\infty} c_m \times R_0(\beta_m, r) \quad \text{in} \quad (a < r < b) \quad (47)$$

This is an expansion of an arbitrary function F(r) defined within the interval (a < r < b) in terms of the Eigen-functions $R_0(\beta_m, r)$ of the eigenvalue problem shown in Eqs. (43)-(45). The unknown coefficient c_m is readily determined by utilizing the orthogonal Eigen-function. The solution can be written as,

$$\psi(r,t) = \sum_{m=1}^{\infty}\left\{\frac{\exp^{-c_{vr}\beta_m{}^2 t}}{N(\beta_m)} R_0(\beta_m, r)\right\}\int_{r'=a}^{r'=b} r' \times R_0(\beta_m, r') \times F(r')dr' \quad (48)$$

where the Eigen-functions $R_0(\beta_m, r)$, Eigen values (β_m) and the norms, $\frac{1}{N(\beta_m)}$

$$R_0(\beta_m, r) = J_0(\beta_m r)Y'_0(\beta_m b) - J'_0(\beta_m b)Y_0(\beta_m r) \quad (49)$$

where, J_0 and Y_0 are known as the Bessel functions of the first and second kinds with order zero [Abramowitz and Stegun (1965)]. In general, the Bessel functions of integer order are the two linearly independent solutions of Bessel's equation

$$\text{where the norms,} \quad \frac{1}{N(\beta_m)} = \frac{\pi^2}{2}\cdot\frac{\beta_m{}^2 J_0{}^2(\beta_m a)}{\left[1-\left(\frac{1}{\beta_m b}\right)^2 J_0{}^2(\beta_m a) - J'_0{}^2(\beta_m a)\right.} \quad (50)$$

and the Eigen values (β_m) are the negative roots of the following transcendental equation

$$J_0(\beta_m a)Y'_0(\beta_m b) - J'_0(\beta_m b)Y_0(\beta_m a) = 0 \quad (51)$$

The solution of the problem stated in Eqs. (39)-(42) in terms of Green's function is given following Eqs. (48)-(51).

$$\psi(r,t) = \int_{r'=a}^{r'=b} r'G(r,t|r',\tau|) \quad F(r')dr' \quad (52)$$
$$\tau=0$$

where r' is the Sturm- Liouville weight function. A comparison of Eqs. (48) and (52) leads to the following:

$$G(r,t|r',\tau|)_{\tau=0} = \frac{\pi^2}{2}\cdot\sum_{m=1}^{\infty}\frac{\beta_m{}^2 J'_0{}^2(\beta_m a)\times\exp^{-C_{vr}\beta_m{}^2 t}}{\left[1-\left(\frac{1}{\beta_m b}\right)^2 J_0{}^2(\beta_m a) - J'_0{}^2(\beta_m a)\right.} \times R_0(\beta_m, r)\times R_0(\beta_m, r') \quad (53)$$

The desired Green's function is obtained by replacing t by (t - τ) in Eq. (53)

$$G(r,t|r',\tau|) = \frac{\pi^2}{2}\cdot\sum_{m=1}^{\infty}\frac{\beta_m{}^2 J'_0{}^2(\beta_m a)\times\exp^{-C_{vr}\beta_m{}^2 (t-\tau)}}{\left[1-\left(\frac{1}{\beta_m b}\right)^2 J_0{}^2(\beta_m a) - J'_0{}^2(\beta_m a)\right.} \times R_0(\beta_m, r)\times R_0(\beta_m, r') \quad (54)$$

Then the solution of the above non-homogeneous problem in terms of this Green's function is given below,

$$\omega(r,t) = \int_{r'=a}^{r'=b} r'G(r,t|r',\tau|) \quad F(r')dr' - \int_{\tau=0}^{t} d\tau \times \int_{r'=a}^{r'=b} r'G(r,t|r',\tau|) \quad R(t)dr' \quad (55)$$
$$\tau=0$$

Introducing the foregoing Green's function into Eq. (55) the solution becomes the following:

$$w(r,t) = -\frac{\pi^2}{2}\cdot\sum_{m=1}^{\infty}\left[\frac{\beta_m{}^2 J'_0{}^2(\beta_m a)\times\exp^{-c_{vr}\beta_m{}^2 t}}{\left[1-\left(\frac{1}{\beta_m b}\right)^2 J_0{}^2(\beta_m a) - J'_0{}^2(\beta_m a)\right.}\right]\times R_0(\beta_m, r) \times \int_{\tau=0}^{t}\exp^{-c_{vr}\beta_m{}^2\tau}\cdot R(\tau)d\tau \int_{r'=a}^{r'=b} r'\times R_0(\beta_m, r')\,dr' \quad (56)$$

where $t = 0$; $\psi = F(r') = 0$

$$R(t) = \frac{A}{t_0\left\{A^2 + 2AB\left(\frac{\tau}{t_0}\right) + \left(B\cdot\frac{\tau}{t_0}\right)^2 + A\left(\frac{\tau}{t_0}\right) + B\left(\frac{\tau}{t_0}\right)^2\right\}} \quad (57)$$

and,

$$\frac{\pi^2}{2}\times\sum_{m=1}^{\infty}\left[\frac{\beta_m{}^2 J'_0{}^2(\beta_m a)\times\exp^{-C_{vr}\beta_m{}^2 t}}{\left[1-\left(\frac{1}{\beta_m b}\right)^2 J_0{}^2(\beta_m a) - J'_0{}^2(\beta_m a)\right.}\right]\times R_0(\beta_m, r) = Q \quad (58)$$

Now applying Eq. (58) into Eq. (56), we get

$$w(r,t) = -Q\int_{\tau=0}^{t}\exp^{-c_{vr}\beta_m{}^2\tau}\cdot R(\tau)d\tau\int_{r'=a}^{r'=b} r'\times R_0(\beta_m, r')\,dr' \quad (59)$$

$$w(r,t) = -\frac{\pi^2}{2}\times\sum_{m=1}^{\infty}\left[\frac{\beta_m{}^2 J'_0{}^2(\beta_m a)\times\exp^{-c_{vr}\beta_m{}^2 t}}{\left[1-\left(\frac{1}{\beta_m b}\right)^2 J_0{}^2(\beta_m a) - J'_0{}^2(\beta_m a)\right.}\right]\times R_0(\beta_m, r)\times \left[\frac{J_1(\beta_m b)}{\beta_m}[bY_1(\beta_m b) - aY_1(\beta_m a)] - \left[\frac{1}{2}Y_1(\beta_m b)\begin{pmatrix}(b)^2\times {}_0\tilde{F}_1\left(;2;-\frac{1}{4}\beta_m{}^2 b^2\right)\\ -(a)^2\times {}_0\tilde{F}_1\left(;2;-\frac{1}{4}\beta_m{}^2 a^2\right)\end{pmatrix}\right]\right]\times \{\log(At_0 + (B+K)t) - \log(At_0 + Bt)\}\exp^{mt} - \exp^{\left(\frac{Amt_0}{B+K}\right)}\begin{Bmatrix}\exp^{m\left(\frac{At_0}{B+K}+t\right)}\log(At_0 + (B+K)t)\\ -E_i\left(m\left(\frac{At_0}{B+K}+t\right)\right)\end{Bmatrix} - \left\{\exp^{\left(\frac{Amt_0}{B+K}\right)}\left\{\exp^{m\left(\frac{At_0}{B+K}\right)}\log(At_0) - E_i\left(m\left(\frac{At_0}{B+K}\right)\right)\right\} + \exp^{mt}\log(At_0 + Bt)\right\} - \left\{\exp^{\left(\frac{-Amt_0}{B}\right)}E_i\left(m\left(\frac{At_0}{B}+t\right)\right) - \log(At_0) + \exp^{\left(\frac{-Amt_0}{B}\right)}E_i\left(m\left(\frac{At_0}{B}\right)\right)\right\} \quad (60)$$

The Puiseux series of $E_i(z)$ is given by Havil (2003)

$$E_i(z) = \gamma + \ln z + z + \frac{1}{4}z^2 + \frac{1}{18}z^3 + \frac{1}{96}z^4 + \frac{1}{600}z^5 \ldots\ldots \quad (61)$$

Here γ = Euler- Mascheroni constant = 5.7721

From Eqs. (29), (48) and (60) the expression for pore water pressure in non-dimensional form is given below.

$$\frac{u}{\sigma'_{vc}} = \left(1 - e^{\sum_{m=1}^{\alpha} w(r,t)}\right)\left(s + \frac{N}{A + B \times N}\right) \quad (62)$$

where,

$$s = \frac{1}{K} = \frac{3}{(1+2k_0)} \quad (63)$$

4.1 Degree of consolidation

$$U_p = \frac{(\sigma' - \sigma'_0)}{(\sigma'_f - \sigma'_0)} = \frac{(u_g - u)}{u_g} \quad (64)$$

The average degree of consolidation defined by effective stress U_{pav} for the entire layer of the soil can be expressed as the following:

$$U_{pav} = 1 - \frac{\left(s + \frac{N}{A + B \times N}\right) \times 2}{(b^2 - a^2) \times \left(\frac{N}{A + B \times N}\right)} \times \int_a^b \left(1 - \exp^{\sum_{m=1}^{\alpha} w(r,t)}\right) r \times dr \quad (65)$$

The degree of consolidation defined by settlement, U_s at depth z can be expressed as

$$U_s = \frac{\log \frac{\sigma'}{\sigma'_0}}{\log \frac{\sigma'}{\sigma'_f}} = \frac{\ln\left(\frac{\sigma'_0 + u_g - u}{\sigma'_0}\right)}{\ln\left(\frac{\sigma'_0 + u_g}{\sigma'_0}\right)} \quad (66)$$

Now integrating the above equation, the average degree of consolidation defined by settlement "U_{sav}" for the entire layer of the soil can be express as

$$U_{sav} = \frac{2}{(a^2 - b^2)} \times \ln N_\sigma \times \int_a^b \ln\left(\frac{\sigma'_0 + u_g - u}{\sigma'_0}\right) \times r \times dr \quad (67)$$

where, $\ln N_\sigma = \ln\left(1 + \frac{u_g}{\sigma'_0} \times K\right)$

The Eqs. (65) and (67) can be solved numerically using Simpson's one-third rule.

5. Model verification

5.1 Pore water pressure with number of cycles

For validation of the proposed analytical model the predicted pore pressure are compared with results of large scale partially drained dynamic tri-axial tests conducted on 300mm diameter by 600mm high reconstituted kaolin soil samples reported by Ni (2012). Vertical and radial pressure in the tri-axial chamber were maintained as 40 kPa and 24 kPa respectively which appeared to simulate soil at a depth of about 4-5 m below ground level. During the tests PVD vertical drain at the center of the soil sample was used to allow radial drainage of water during consolidation under cyclic loading. Miniature pore pressure transducers were fixed in kaolin soil at different pre-defined positions to measure pore pressure developed during cyclic loading. A schematic diagram for the sample showing the position of vertical radial drains and pore pressure transducers are shown in Fig. 6. The relevant parameters for soil, cyclic load and vertical drains adopted in this analysis are furnished in Table 1.

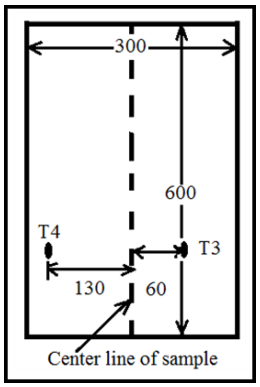

Fig. 6 Soil sample diagram along with pore pressure transducers (all units are in mm)

Table 1 Laboratory test data of drained cyclic loading [Ni (2012)]

Specimen	I_p (%)	Cyclic stress ratio (CSR)	Frequency, (F_z) (H_z)
D_{01}	28	0.4	1.0
D_{04}	28	0.8	0.1

Parameters for radial consolidation (PVDs):

- Equivalent radius of PVD (a) = 16.55 mm
- Radius of influence zone (b)= 150 mm
- Coefficient of consolidation in a horizontal direction (c_{vr}) = 9.46 m^2/year

The normalized pore pressure ratio predicted for the partially drained cyclic load tests with PVDs are given in Figs. 7 and 8 respectively. 'E' refers to the experimental and 'P' to the proposed predicted results. The transducers were provided at a distance of 60 mm and 130 mm from the center line of the sample (Fig. 6). Figs. 7 and 8 show that for transducer at a distance 130 mm the recorded results are in close agreement to the predicted values. However in Fig. 7, the predicted data recorded at 60 mm distance shows that the pore pressure ratio dissipates rapidly due to the availability of drainage at closer vicinity. For the transducer at 130mm from the center of the cell, magnitude of pore water pressure is comparatively higher due to greater length of drainage path. Further, the trends of predicted pore pressure do not match with the experimental results for the transducer located at 60mm from the vertical drain. This deviation may be attributed to no smear condition of the proposed model. Fig. 8 shows that the sample failed after 3000 cycles when the critical pore pressure is 0.68 at cyclic shear stress of 0.8 and frequency 0.1 at a distance of 130 mm from the PVD drain for experimental and proposed

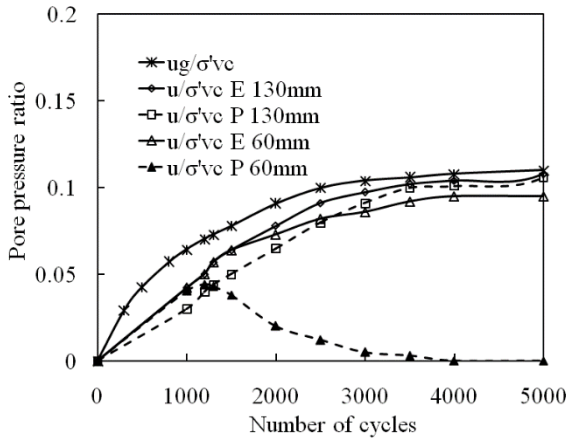

Fig. 7 Variation of pore pressure ratio with number of cycles for F_z 1.0 H_z [Data source: Ni (2012)]

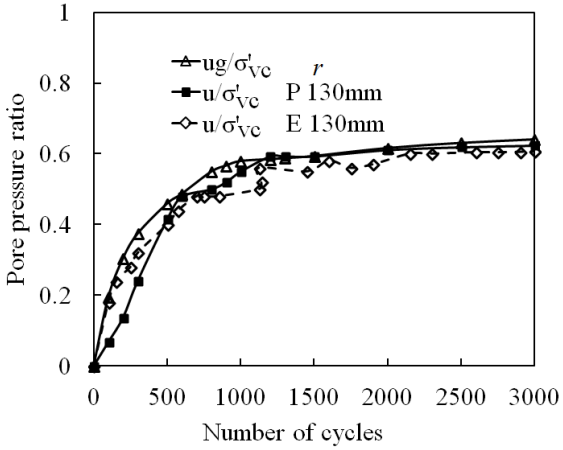

Fig. 8 Variation of pore pressure ratio with number of cycles for F_z 0.1 H_z [Data source: Ni (2012)]

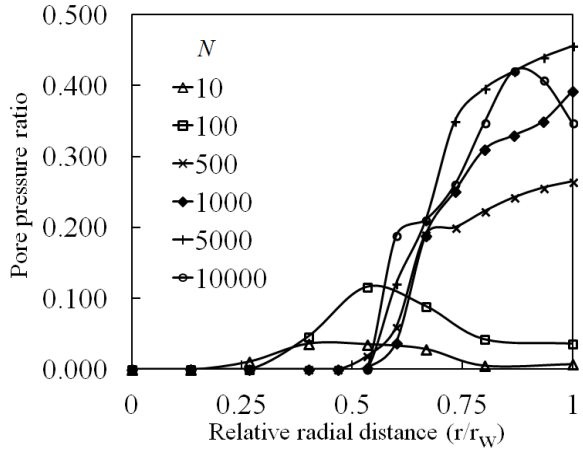

Fig. 9 Variation of pore pressure ratio with relative radial distance for different number of cycles for F_z 0.1 H_z [Data source: Ni (2012)]

results. Thus the frequency of cyclic load affects the pore water accumulation in soil sample as its magnitude increased with the reduction in F_z from 1.0 H_z to 0.1 H_z which is clearly visible in Figs. 7 and 8 and the predicted

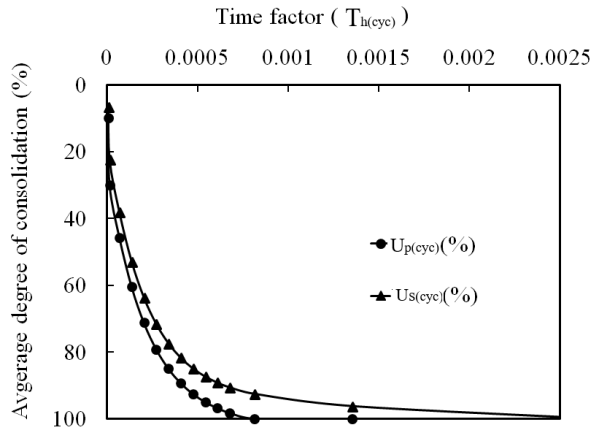

Fig. 10 Average degree of consolidation defined by effective stress and pore water pressure with time factor for CSR= 0.4, I_p = 28 and F_z = 1.0 H_z [Data source: Ni (2012)]

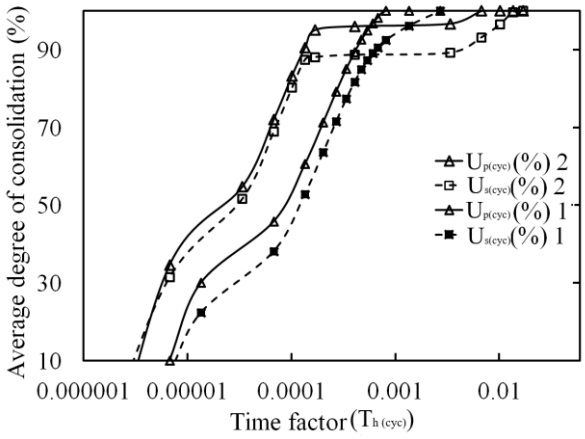

Fig. 11 Average degree of consolidation defined by effective stress and pore water pressure with time factor for CSR = 0.4, I_p = 28 and F_z = 1.0 and 2.0 H_z [Data source: Ni (2012)]

pore pressure are in good agreement with the measured values.

Further, Fig. 9 shows the pore pressure distribution measured along the radial distance which varies from center of PVDs to outer diameter of sample for CSR = 0.8 and F_z = 0.1 H_z. Generated undrained pore pressure dissipates through the PVDs under cyclic loading. The figure shows that when the number of cycles are less (N = 10, 100), the magnitude of pore water pressure generation is very slow followed by rapid subsequent dissipation near the inner boundary. For higher cycles (N ≥ 500) the pore pressure accumulates near the outer boundary and dissipates through the vertical drains inserted at the center of the specimen. Maximum pore pressure at outer periphery (r/r_w =1) is achieved for 5000 cycles. It is interesting to note that for greater number of cycles (N = 10000) the pore pressure declined at the outer edges.

5.2 Average degree of consolidation

Figs. 10 and 11 depict the average degree of

Table 2 Case study input parameters*

Type of soils	Sub layer thickness (m)	CSR	C_c	σ'_{vc} (kPa)	F_z (H_z)	e_0	c_{vr} (m^2/year)
Ballast and fill	1	1.25	0.91	6.20	5-10	2.26	
Soil 1	1	1.25	0.92	11.99	5 - 10	2.26	6 -12
	1	1.25	0.93	17.78			
	1	1.25	0.94	23.58			
	1	1.25	0.95	29.37			
	1	1.25	0.96	35.16			
	1	1.10	0.97	40.96			
	1	0.95	0.98	46.75			
	1	0.90	0.99	52.54			
	1	0.65	1.00	58.34			
Soil 2	1	0.50	1.00	64.03	5 - 10	2.26	2-4
	1	0.51	1.01	70.54			
	1	0.52	1.02	76.74			
	1	0.53	1.03	82.95			
	1	0.54	1.04	89.15			
	1	0.55	1.05	95.36			
	1	0.56	1.06	101.56			
	1	0.57	1.07	107.76			
	1	0.50	1.08	113.97			
	1	0.59	1.09	120.17			

Unit weight varies from 14 - 16 kN/m^3

Undrained shear strength varies from 10 - 40 kPa

Over consolidation ratio varies from 1 - 1.2

*(Original data from Indraratna *et al.* (2010)

consolidation in terms of both effective stress ($U_{p(cyc)}$, %) and settlement ($U_{s(cyc)}$, %) with time factors ($T_{h(cyc)}= c_{vr}t/d^2$) for frequencies 1.0H_z and 2.0H_z , CSR= 0.4, I_p=28 under long term cyclic loading. These figures show that $U_{s(cyc)}$ for different frequencies are lesser than that of $U_{p(cyc)}$ and both $U_{p(cyc)}$ and $U_{s(cyc)}$ attain identical values at $T_{h(cyc)}=$ 0.0025.

6. Design example

The proposed radial consolidation model can be used to predict consolidation settlement of cohesive deposits under long-term cyclic load. Here, a case study from Ni (2012) on deformation behavior of soil of an existing railway track at Sandgate in Australia has been used to determine the settlement of soil using the proposed formulation and are also compared with the reported field data.

6.1 Problem

The Sandgate Rail Grade Separation Project located at Sandgate (near Wollongong) was subjected to a cyclic deviator stress of 50 to 100 kPa and load frequency of 5 to 10 H_z due to approach speed of 100 km/h for freight train. The ground water table was located at the ground surface and the water content of soil layers was very close to their liquid limits. The subsoil stratification along with in-situ soil properties and other input parameters with depths varying from 0 to 20 m is presented in Fig. 12 and Table 2.

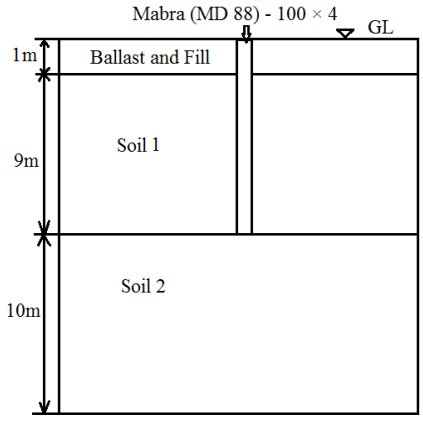

Fig. 12 Unit cell of radial consolidation with three layer formation of soil

The corresponding design axle load (P_d) can then be obtained from the Australian standards [AS 1085.14-1997] as referred by Ni (2012),

$$P_d = \left(1 + 5.4\frac{V}{D}\right) P_s$$

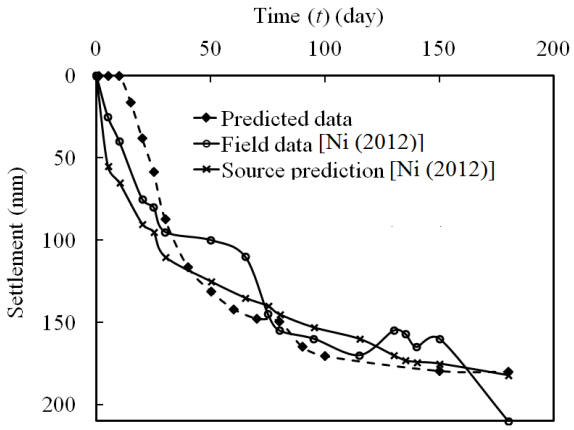

Fig. 13 Comparison of settlement under traffic loading with field data of Ni (2012)

where, V = 40 km/h is train speed, D = 860 mm is the diameter of the wheel, and P_s = 25 tons is the axle load.
The PVDs were installed at 2 m apart to effectively accelerate the dissipation of excess pore pressure due to the train load and enhance the stability of the newly constructed rail track. The PVDs were 8 m long, as the train load likely to be restricted to a depth of 5 - 8 m. Mebra (MD 88) vertical drains (100 mm × 4 mm) were installed to accelerate the consolidation of soil deposits.

- Radius of influence = b = 0.564 × S_D = 1.128 m (Square pattern)
- Equivalent diameter = $d_e = 0.5w + 0.7t$ (Long and Covo, 1994) = 0.0264 m
- Equivalent radius = a = 0.0132 m
- Coefficient of radial consolidation = c_{vr} = 12 m^2/year
- Degree of consolidation = U= 1-(1-U_z)(1-U_r), here [U_z = 0]

The predicted settlement of the constructed rail track with time is furnished in Fig. 12 and compared with measured settlement and predicted values reported by Ni (2012). The figure indicates that the proposed generalized solution show very good accuracy in reproducing the traffic-load-induced settlement of the railway track.

7. Conclusions

This paper proposed a closed-form analytical solution to predict one dimensional consolidation under cyclic load using separation of variables and Green's functions techniques. The conclusions drawn from this study are as follows:

• The generation of excess pore pressure coupled with subsequent dissipation in soil deposits has been derived by using a modified non-linear axisymmetric radial consolidation expression based on Davis and Raymond's (1965) basic assumption and undrained pore pressure generation model proposed by Paul *et al.* (2015).

• It is observed that pore pressure accumulation increases initially followed by dissipation at higher number of loading cycles through vertical drains. However at outer boundaries the pore pressure generates slowly during initial phase of load application reaches maximum at substantially higher number of cycles.

• The effect of frequency of cyclic loading is significant from the early stages of consolidation. The higher frequencies cause reduction in excess pore water pressure accumulation in the soil.

• The application of the proposed analytical model to the real life problems establishes its efficiency in predicting deformation behavior using model output when compared with experimental data and case study outputs. This proposed model is therefore a useful and practical tool for predicting soil behavior during radial consolidation under cyclic loading.

References

Abramowitz, M. and Stegun, I.A. (1964), *Handbook of Mathematical Functions with Formulas, Graphs, and Mathematical Tables*, National Bureau of Standards Applied Mathematics Series, U.S. Government Printing Office, Washington D.C., U.S.A.

Amiri, A., Toufigh, M.M., Sadeghi Janat Abadi, S. and Toufigh, V. (2018), "Comparison of radial consolidation behavior of clay under three types of cyclic loading", *Civ. Eng. Infrastruct. J.*, **51**(1), 17-33. https://doi.org/10.7508/CEIJ.2018.01.002.

Ansal, A.M. and Erken, A. (1989), "Undrained behavior of clay under cyclic shear stresses", *J. Geotech. Eng.*, **115**(7), 968-983. https://doi.org/10.1061/(ASCE)0733-9410(1989)115:7(968).

Attya, A., Indraratna, B. and Rujikiatkamjorn, C. (2007), "Effectiveness of vertical drains in dissipating excess pore pressures induced by cyclic loads clays", *Proceedings of the 16th Southeast Asian Geotechnical Conference*, Selangor, Malaysia, May.

Bai, B. and Shi, X. (2017), "Experimental study on the consolidation of saturated silty clay subjected to cyclic thermal loading", *Geomech. Eng.*, **12**(4), 707-721. https://doi.org/10.12989/gae.2017.12.4.707.

Carslaw, H.S. and Jaeger, J.C. (1959), *Conduction of Heat in Solids*, Oxford University Press, London, U.K.

Conte, E. and Troncone, A. (2006), "One dimensional consolidation under general time-dependent loading", *Can. Geotech. J.*, **43**, 1107-1116. https://doi.org/10.1139/t06-064.

Conte, E. and Troncone, A. (2007), "Nonlinear consolidation of thin layers subjected to time dependent loading", *Can. Geotech. J.*, **44**, 717-725. https://doi.org/10.1139/t07-015.

Conte, E. and Tronecone, A. (2009), "Radial consolidation with vertical drains and general time-dependent loading", *Can. Geotech. J.*, **46**, 25-36. https://doi.org/10.1139/T08-101.

Das, B. (1985), *Advanced Soil Mechanics*, McGraw-Hill, New York, U.S.A.

Davis, E.H. and Raymond, G.P. (1965), "A non linear theory of consolidation", *Géotechnique*, **15**(2), 161-173. https://doi.org/10.1680/geot.1965.15.2.161.

De Alba, P., Seed, H.B. and Chan, C.K. (1976), "Sand liquefaction in large scale simple shear tests", *J. Geotech. Div.*, **102**, 909-928. https://doi.org/10.1080/19386362.2019.1701219.

Deng, Y.B., Xie, K.H., Lu, M.M., Tao, H.B. and Lu, G.B. (2013), "Consolidation by prefabricated vertical drains considering the time dependent well resistance", *Geotext. Geomembranes*, **36**(1), 20-26. https://doi.org/10.1016/j.geotexmem.2012.10.003.

Havil, J. (2003), *Gamma Exploring Euler's Constant*, Princeton University Press, Princeton, New Jersey, U.S.A.

Hsu, T.W. and Liu, H.Y. (2013), "Consolidation for radial drainage under time-dependent loading", *J. Geotech. Geoenviron. Eng.*,

139(12), 2096-2103. https://doi.org/10.1061/(ASCE)GT.1943-5606.0000942.

Hyodo, M., Yasuhara, K. and Murata, H. (1988), "Earthquake induced settlements in clays", *Proceedings of 9th World Conference on Earthquake Engineering*, Tokyo-Kyoto, Japan, August.

Indraratna, B., Attya, A. and Rujikiatkamjorn, C. (2009), "Experimental investigation on effectiveness of a vertical drain under cyclic loads", *J. Geotech. Geoenviron. Eng.*, **135**(6), 835-839. https://doi.org/10.1061/(ASCE)GT.1943-5606.0000006.

Indraratna, B., Kan, M.E., Potts, D., Rujikiakatamjorn, C. and Sloan, S.W. (2016), "Analytical solution and numerical simulation of vacuum consolidation by vertical drains beneath circular embankments", *Comput. Geotech.*, **80**, 83-96. https://doi.org/10.1016/j.compgeo.2016.06.008.

Indraratna, B. and Redana, I.W. (2000), "Numerical modeling of vertical drains with smear and well resistance installed in soft clay", *Can. Geotech. J.*, **37**(1), 132-145. https://doi.org/10.1139/t99-115.

Indraratna, B.N., Rujikiatkamjorn, C., Ewers, B. and Adams, M. (2010), "Class A prediction of the behavior of soft estuarine soil foundation stabilised by short vertical drains beneath a rail track", *J. Geotech. Geoenviron. Eng.*, **136**(5), 686-696. https://doi.org/10.1061/(ASCE)GT.1943-5606.0000270.

Kelly, R. (2014), "Assessment of smear parameters for use in wick drain design", *Proc. Inst. Civ. Eng. Ground Improv.*, **167**(3), 186-191. https://doi.org/10.1680/jgrim.15.00034.

Lambe, T.W. and Whitman, R.V. (1969), *Soil Mechanics*, John Wiley and Sons, Inc., New York, U.S.A.

Lancellotta, R. (1995), *Geotechnical Engineering*, Balkema, Rotterdam, The Netherlands.

Lekha, K.R., Krishnaswamy, N.R. and Basak, P. (1998), "Consolidation of clay by sand drains under time-dependent loading", *J. Geotech. Geoenviron. Eng.*, **124(**1), 91-94. https://doi.org/10.1061/(ASCE)1090-0241(1998)124:1(91).

Leo, C.J. (2004), "Equal strain consolidation by the vertical sand drains", *J. Geotech. Geoenviron. Eng.*, **130(**3), 316-327. https://doi.org/10.1061/(ASCE)1090-0241(2004)130:3(316).

Li, C., Huang, J., Wu, L., Lu, X. and Xia, C. (2018), "Approximate analytical solutions for one-dimensional consolidation of a clay layer with variable compressibility and permeability under a ramp loading", *Int. J. Geomech.*, **18**(11), 06018032. https://doi.org/10.1061/(ASCE)GM.1943-5622.0001296.

Long, R.P. and Covo, A. (1994), "Equivalent diameter of vertical drains with an oblong cross section", *J. Geotech. Eng.*, **120**(9), 1625-1630. https://doi.org/10.1061/(ASCE)0733-9410(1994)120:9(1625).

Lu, M., Xie, K. and Wang, S. (2011), "Consolidation of vertical drain with depth-varying stress induced by multi-stage loading", *Comput. Geotech.*, **38,** 1096-1101. https://doi.org/10.1016/j.compgeo.2011.06.007.

Matsui, T., Ohara, H. and Ito, T. (1980), "Cyclic stress-strain history and shear characteristics of clay", *J. Geotech. Eng.*, **106** (GT10), 1101-1120. https://doi.org/10.1061/AJGEB6.0001043.

Ma, B.H, Hu, Z.Y., Li, Z, Cai, K., Zhao, M.H., He, C.B. and Huang X.C. (2020), "Finite difference method for the one-dimensional non-linear consolidation of soft ground under uniform load", *Front. Earth Sci.*, **8**, 111. https://doi.org/10.3389/feart.2020.00111.

Ni, J. (2012), "Application of geosynthetic vertical drains under cyclic loads in stabilizing tracks", Ph.D. Dissertation, University of Wollongong, Wollongong, Australia.

Ni, J., Indraratna, B., Geng, X.Y., Carter, J.P. and Chen, Y.L. (2014), "Model of soft soils under cyclic loading", *Int. J. Geomech.*, **15**(4), 04014067. http://doi.org/10.1061/ (ASCE) GM.1943- 5622.0000411.

Ohara, S. and Matsuda, H. (1988), "Study on the settlement of saturated clay layer induced by cyclic shear", *Soils Found.*, **28**(3), 103-113. https://doi.org/10.3208/sandf1972.28.3_103.

Paul, M. and Sahu, R.B. (2012). "One dimensional consolidation under cyclic loading", *Int. J. Geotech. Eng.*, **6**, 395-401. https://doi.org/10.3328/IJGE.2012.06.03.395-402.

Paul, M., Sahu, R.B. and Banerjee, G. (2015), "Undrained pore pressure prediction in clayey soil under cyclic loading", *Int. J. Geomech.*, **15**(5), 04014082(11). https://doi.org/10.1061/(ASCE)GM.1943-5622.0000431.

Paul, M., Sahu, R.B. and Banerjee, G. (2019), "A generalized consolidation model under cyclic loading", *Int. J. Geotech. Eng.*, **14**(5) 497-513. https://doi.org/10.1080/19386362.2019.1701219.

Prakasha, K.S. and Chandrasekaran, V.S. (2005), "Behavior of marine sand-clay mixtures under static and cyclic triaxial shear", *J. Geotech. Geoenviron. Eng.*, **131**(2), 213-222. https://doi.org/10.1061/(ASCE)1090-0241(2005)131:2(213).

Samang, L., Miura, N. and Sakai, A. (2005), "Long term measurement of traffic load induced settlement of pavement surface in saga airport highway, Japan", *Journal Teknik Sipil*, **12**(4), 275-286. http://doi.org/10.5614%2Fjts.2005.12.4.5.

Seed, H.B. and Idriss, I.M. (1971), "Simplified procedure for evaluating soil liquefaction potential", *J. Soil Mech. Found. Div. Proc. Amer. Soc. Civ. Eng.*, **97**(SM9), 1249-1273.

Smith, G.N. and Smith, I.G. (1998), *Elements of Soil Mechanics*, Blackwell, London, U.K.

Tang, X.W. and Onitsuka, K. (2000), "Consolidation by vertical drains under time dependent loading", *Int. J. Numer. Anal. Met. Geomech.*, **24**(9), 739-751. https://doi.org/10.1002/1096-9853(20000810)24:9<739::AID-NAG94>3.0.CO;2-B.

Van Eekelen, H.A.M. and Potts, D.M. (1978), "The behavior of drammen clay under cyclic loading", *Geotechnique*, **28**(2), 173-196. https://doi.org/10.1680/geot.1978.28.2.173.

Walker, R. and Indraratna, B, (2006), "Vertical drain consolidation with parabolic distribution of permeability in smear zones", *J. Geotech. Geoenviron. Eng.*, **132**(7), 937-941. https://doi.org/10.1061/(ASCE)1090-0241(2006)132:7(937).

Walker, R. and Indraratna, B. (2009), "Consolidation analysis of a stratified soil with vertical and horizontal drainage using the spectral method", *Geotechnique*, **59**(5), 439-449. https://doi.org/10.1680/geot.2007.00019.

Wilson, N. and Elgohary, M. (1974), "Consolidation of soils under cyclic loading", *Can. Geotech. J.*, **11**, 420-423. https://doi.org/10.1139/t74-042.

Yasuhara, K., Sate, K., Zen, K., Yamazaki, H., Hyodo, M. and Yamamoto, T. (1995), "Settlement observation and its prediction of a breakwater at Tottori port", *Proceedings of the International Symposium on Compression and Consolidation of Soft Clays Soils*, Japan, January.

Yazdani, H. and Toufigh, M.M. (2012), "Nonlinear consolidation of soft clays subjected to cyclic loading - Part I: theory." *Geomech. Eng.*, **4**(4), 229-241. https://doi.org/10.12989/gae.2012.4.4.229.

Yoshikuni, H. and Nakanodo, H. (1974), "Consolidation of soils by vertical drain wells with finite permeability", *Soils Found.*, **14**, 35-46. https://doi.org/10.3208/sandf1972.14.2_35.

Zhu, G.F. and Yin, J.H. (2001), "Consolidation of soil with vertical and horizontal drainage", *Geotechnique*, **51**(4), 361-367. https://doi.org/10.1680/geot.2001.51.4.361.

Zhang, Y., Wu, W., Mei, G. and Duan, L. (2019), "Three-dimensional consolidation theory of vertical drain based on continuous drainage boundary", *J. Civ. Eng. Manage.*, **25**(2), 145-155. https://doi.org/10.3846/jcem.2019.8071.